



THE EFFECT OF NON-LINEARITY OF RAILWAY TRACKS ON GROUND-BORNE VIBRATION

Samuel Koroma, Mohammed Hussein, David Thompson *and* Evangelos Ntotsios

Institute of Sound and Vibration Research, University of Southampton, Highfield, Southampton, United Kingdom SO17 1BJ,

e-mail: S.G.Koroma@soton.ac.uk

The type of railpad model adopted in modelling the dynamic behaviour of a railway track influences the accuracy of prediction of the vibration of the track, as well as the forces transmitted to the ground. The linear Kelvin-Voigt model is most widely used amongst authors. This model consists of a parallel arrangement of spring and viscous dashpot, representing the linear stiffness and damping properties of the railpad respectively. However, railpads have been found to exhibit strong nonlinearity with preload and frequency dependent properties.

In this paper, preliminary results of the work undertaken as part of the MOTIV (Modelling Of Train Induced Vibration) project on nonlinearity of tracks are presented. This work focuses on the effect of nonlinearity of railpads. A model of a rail that is discretely supported on railpads is formulated in the time domain. The railpads are modelled as a nonlinear Kelvin-Voigt material with preload dependent stiffness and damping properties. The model is subjected to a moving load with combined static and dynamic parts, and is solved independently to calculate the forces transmitted through the railpads. These are then used as inputs to a separate floating slab/ground system, which is formulated in the wavenumber-frequency domain, to study the effect of nonlinearity on ground vibration. This method is termed weak coupling, since the effect of the interaction between the rail-railpads and the slab-ground system is neglected.

Results are presented as frequency spectra for the ground displacements under and at a distance from the track. A comparative study of the results for both linear and nonlinear cases is conducted for three preload levels on the track. The inclusion of railpad nonlinearity into the modelling results in up to 6 dB differences in peak displacement over a frequency range of 0-200 Hz compared to a linear model, for the parameters used.

1. Introduction

The effects of railpad nonlinearity on railway track dynamics have been studied by Wu and Thompson [1] and more recently by Koroma et al. [2, 3] for stationary harmonic loads. Moving load cases are also considered in Koroma [4]. However, these models only focused on effects of preload/ nonlinearity on track dynamics and forces transmitted through the railpads, without further investigating the subsequent effects on ground-borne vibration.

This paper considers the coupling of the nonlinear discretely supported rail model from [2] to a slab-ground system in order to investigate the effect of railpad nonlinearity on ground-borne vibration. The coupling is done using a weak formulation, in which the rail-railpad system is solved independently of the presence of the slab-ground system, to calculate the forces transmitted through

the railpads. These are then transformed to the wavenumber domain and used as input to the slab-ground model. The method of coupling of the slab and the ground follows a similar approach to that presented in [5].

The model is presented in Section 2. For linear cases, the modelling is carried out in the wavenumber-frequency domain as described in Section 2.1, using strong and weak coupling approaches. For the nonlinear case, however, the analysis is carried out in the space-time domain as described in Section 2.2. Some example results are presented in Section 3 and the conclusions given in Section 4.

2. Model formulation

This section describes the formulation of a slab-track-ground model. Two approaches, strong and weak coupling, are followed in coupling the rail-railpad system to the slab-ground system. In strong coupling, the differential equations of motion are formulated with full interaction existing between all components of the slab-track-ground system. The weak coupling approach, on the other hand, assumes that the forces transmitted to the slab are mainly controlled by the rail-railpad system, since the stiffness of the slab-ground system is much greater than that of the rail-railpad system. Hence, the rail-railpad system can be uncoupled from the slab-ground system and solved independently for the purpose of calculating the forces transmitted through the railpads. These forces are then applied as input to the slab-ground model. This assumption is more reliable when the stiffness of the slab-ground system is much greater than that of the railpads. It also allows for the inclusion of railpad nonlinearity into the formulation without the complication of modelling the ground in the time domain.

The analysis is carried out entirely in the wavenumber-frequency domain for the strong coupling and linear weak coupling cases. However, time domain analysis is used when nonlinear railpads are included in the rail-railpad system, in order to calculate the forces transmitted through the railpads. These are then transformed to the wavenumber-frequency domain and used as input to slab-ground model. The wavenumber-frequency domain model is discussed in Section 2.1.1 and the time domain one in Section 2.2.

2.1 2.5D models in the wavenumber-frequency domain

Fig. 1 shows the coupling of a rail to a slab-ground model using strong and weak coupling approaches. The forces and displacements are in the wavenumber domain, signified by $(\hat{\cdot})$, such that for a function $g(x)$

$$g(x) = \frac{1}{2\pi} \int_{-\infty}^{\infty} \hat{g}(\xi) e^{i\xi x} d\xi \quad \text{and} \quad \hat{g}(\xi) = \int_{-\infty}^{\infty} g(x) e^{-i\xi x} dx. \quad (1)$$

Equation (1) is the Fourier transform pair relating the space, x , and the wavenumber, ξ , domains; where $\xi = 2\pi/\lambda$, with λ the wavelength of each harmonic component of g .

In both the weak and strong coupling cases, the rail and slab are modelled as Euler-Bernoulli beams of mass, M_r and M_s , per unit length and bending stiffness, EI_r and EI_s respectively. The rail is connected to the slab through railpads with dynamic stiffness, \bar{K}_{rs} , per unit length, whereas the slab and ground are connected through slab bearings with dynamic stiffness, \bar{K}_{sg} , per unit length. The rail is subjected to a force \hat{P} in the wavenumber domain.

For the purpose of coupling the slab to the ground, it is assumed that the slab is rigid in the y -direction and the ground displacement is constant across its width. Hence the ground displacement at the centre of the track, $U_g(\xi, y = 0)$, will be used for coupling the slab to the ground.

The strong coupling case is presented in Section 2.1.1 and the weak coupling case in Section 2.1.2.

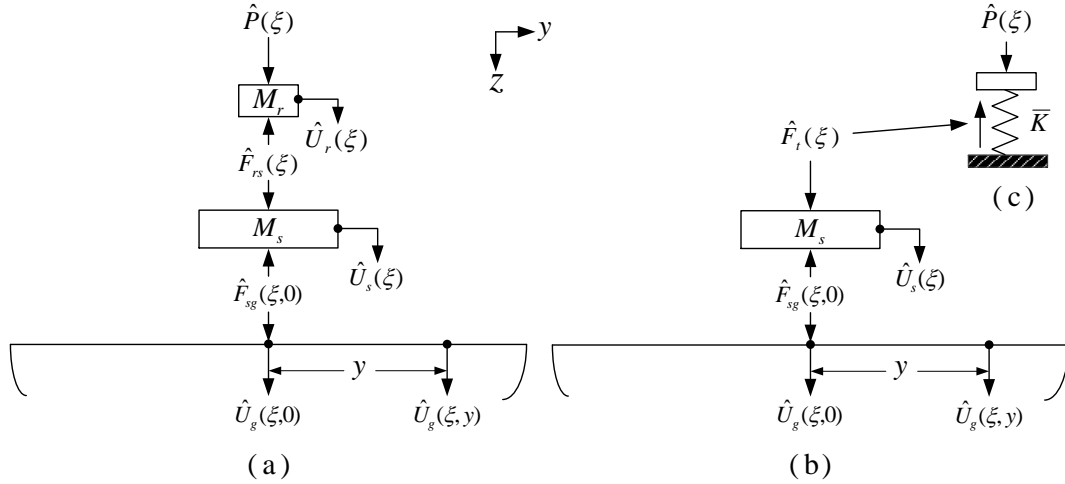


Figure 1: Coupling of the slab track-ground system in the wavenumber- domain using (a) strong coupling and (b) weak coupling and (c) sub-model for calculating \hat{F}_t ; cross section along the $y - z$ plane of the 3D model

2.1.1 Strong coupling between the rail-railpad and slab-ground models

In the strong coupling case in Fig. 1(a), the slab interacts with the rail through the interaction force in the railpads, \hat{F}_{rs} , and with the ground through the force, \hat{F}_{sg} . Expressions for these forces are given by

$$\hat{F}_{rs}(\xi) = \bar{K}_{rs} \left(\hat{U}_r(\xi) - \hat{U}_s(\xi) \right), \quad (2a)$$

$$\hat{F}_{sg}(\xi, y = 0) = \bar{K}_{sg} \left(\hat{U}_s(\xi) - \hat{U}_g(\xi, y = 0) \right), \quad (2b)$$

where $\bar{K}_{rs} = K_{rs} + i\omega_0 C_{rs}$ for a Kelvin-Voigt model of stiffness, K_{rs} , and damping C_{rs} , for $\omega_0 = 2\pi f_0$, f_0 being the excitation frequency. Similarly, $\bar{K}_{sg} = K_{sg} + i\omega_0 C_{sg}$ for the slab bearings.

The equilibrium conditions can be written for the rail, taking into account the expressions in Eq. (2), as

$$(1 + \bar{K}_{rs} \hat{H}_r) \hat{U}_r - \bar{K}_{rs} \hat{H}_r \hat{U}_s = \hat{H}_r \hat{P}, \quad (3)$$

and similarly for the slab as

$$\left(1 + (\bar{K}_{rs} + \bar{K}_{sg}) \hat{H}_s \right) \hat{U}_s - \bar{K}_{rs} \hat{H}_s \hat{U}_r - \bar{K}_{sg} \hat{H}_s \hat{U}_g(\xi, 0) = 0, \quad (4)$$

where \hat{H}_r and \hat{H}_s are the transfer functions of the rail and slab respectively and are given by

$$\hat{H}_r(\xi) = \frac{1}{EI_r \xi^4 - M_r (\omega_0 - \xi v)^2}, \quad \hat{H}_s(\xi) = \frac{1}{EI_s \xi^4 - M_s (\omega_0 - \xi v)^2}. \quad (5)$$

The displacement of a point on the ground, $\hat{U}_g(\xi, y)$ at a distance y from the centre due to a uniform strip load of width $2B$ and magnitude $1/2B$ distributed symmetrically about $y = 0$, can be calculated, using the Green's function for a homogeneous halfspace [6], as the product of the transfer function of the ground, $\hat{H}_g(\xi)$, and the force, $\hat{F}_{sg}(\xi, y = 0)$. Now $\hat{H}_g(\xi) = \hat{H}'_g(\xi, y = 0) \sin(\gamma B) / \gamma B$, where $\hat{H}'_g(\xi, y = 0)$ is the corresponding transfer function due to a unit point load at the origin.

The transfer functions of the ground in the wavenumber domain, $\hat{H}'_g(\xi, \gamma)$, are calculated for a unit load acting downwards at $y = 0$, where γ is the wavenumber in the y -direction. To calculate $\hat{H}'_g(\xi, y)$, therefore, the inverse Fourier transformation from the γ domain to the y domain should

be calculated as in Eq. (1). However, due to symmetry of $\tilde{H}'_g(\xi, \gamma)$ in the γ domain, this computation can be done using only positive wavenumbers. Therefore, $\hat{H}_g(\xi, y)$ for the strip load can be obtained as

$$\hat{H}_g(\xi, y) = \frac{1}{\pi} \int_0^{\infty} \tilde{H}'_g(\xi, \gamma) \frac{\sin(\gamma B)}{\gamma B} \cos(\gamma y) d\gamma. \quad (6)$$

For the coupling at the slab-ground interface, the ground displacement at the origin, $\hat{U}_g(\xi, 0)$ can be obtained, using expression for $\hat{F}_{sg}(\xi, y = 0)$ in Eq. (2), from

$$\left(1 + \bar{K}_{sg} \hat{H}_g(\xi, y)\right) \hat{U}_g(\xi, y = 0) = \bar{K}_{sg} \hat{H}_g(\xi, y) \hat{U}_s, \quad |y| \leq B. \quad (7)$$

By substituting for $\hat{U}_g(\xi, y = 0)$ from Eq. (7) and into Eq. (4), and arranging the resulting equation and Eq. (3) into a matrix form, we get

$$\begin{bmatrix} 1 + \bar{K}_{rs} \hat{H}_r & -\bar{K}_{rs} \hat{H}_r \\ -\bar{K}_{rs} \hat{H}_s & 1 + \left(\bar{K}_{rs} + \bar{K}_{sg} + \frac{\bar{K}_{sg}^2 \hat{H}_g}{1 + \bar{K}_{sg} \hat{H}_g} \right) \hat{H}_s \end{bmatrix} \begin{Bmatrix} \hat{U}_r \\ \hat{U}_s \end{Bmatrix} = \begin{Bmatrix} \hat{H}_r \hat{P} \\ 0 \end{Bmatrix}, \quad (8)$$

Equation (8) can be solved for the unknown displacements, \hat{U}_r and \hat{U}_s , from which the ground displacement $\hat{U}_g(\xi, y = 0)$, and the reaction forces \hat{F}_{rs} and $\hat{F}_{sg}(\xi, y = 0)$ can be obtained. Furthermore, $\hat{F}_{sg}(\xi, y = 0)$ can then be used as input to the ground to calculate its response at any distance y away from the centreline of the track.

2.1.2 Weak coupling between the rail-railpad and slab-ground models

In this section, the case of weak coupling depicted in Fig. 1(b) is considered. The same slab-ground system is subjected to an external force, \hat{F}_t , which can take any arbitrary form. For this application, however, \hat{F}_t is the transformed transmitted force from a rail-railpad model which is solved independently.

Now the displacement of the slab is given by

$$\hat{U}_s = \hat{H}_s \left(\hat{F}_t - \hat{F}_{sg}(\xi, y = 0) \right), \quad (9)$$

whereas that of a point on the ground at the origin by

$$\hat{U}_g(\xi, y = 0) = \hat{H}_g(\xi, y) \hat{F}_{sg}(\xi, y = 0). \quad (10)$$

By substituting for \hat{U}_s and $\hat{U}_g(\xi, y = 0)$ from Eqs. (9) and (10) and into Eq. (2b), the interaction force at the slab-ground interface can be calculated as

$$\hat{F}_{sg}(\xi, y = 0) = \frac{\bar{K}_{sg} \hat{H}_s \hat{F}_t}{1 + \bar{K}_{sg} \left(\hat{H}_s + \hat{H}_g(\xi, y) \right)}. \quad (11)$$

Consider the case of a rail continuously supported on a layer of railpad with linear stiffness and damping properties, and subjected to a harmonic load moving with speed, v . The reaction force in the railpad, which is in turn transmitted to the slab-ground system, can be calculated by solving the track model independently as

$$\hat{F}_t(\xi) = \frac{\bar{K}_{rs}}{EI_r \xi^4 - M_r (\omega_0 - \xi v)^2 + \bar{K}_{rs}}. \quad (12)$$

By substituting Eq. (12) into Eq. (11), $\hat{F}_{sg}(\xi, y = 0)$ can be obtained. The calculation for ground vibration follows the same approach as for the strong coupling case.

For a nonlinear railpad layer, on the other hand, the analysis of the track vibration needs to be carried out in the time domain. This is described in Section 2.2.

2.2 FE model in the space-time domain

This section deals with the formulation of a discretely supported rail model in the time domain. The rail is discretised into N finite elements of length, L , each modelled as an Euler-Bernoulli beam, and is supported on equally spaced railpads (at regular interval of 0.6 m). The railpads are in turn resting on a rigid foundation. For the current study, 360 elements of length 0.3 m are used in the computation. The railpads are modelled as nonlinear with preload dependent behaviour [2]. The model is subjected to a load with combined static and dynamic parts, $P_{tot}(x, t) = P_0 + P_1 e^{i\omega_0 t}$, moving on the rail at a constant speed, v ; where P_0 and P_1 are the static preload and dynamic force amplitude respectively, and $x = vt$ corresponds to the position of the load at any instant, t . The model is used to calculate the space-time domain reaction force matrix of the railpads. This is then transformed to the wavenumber-frequency domain, and used as input to the slab-ground model described in Section 2.1.2 for the purpose of calculating ground vibration.

The space-discretised ordinary differential equation that governs the dynamic behaviour of the rail-railpad system can be written as

$$\mathbf{M}\ddot{\mathbf{U}}_r + \mathbf{C}\dot{\mathbf{U}}_r + \mathbf{K}\mathbf{U}_r = \mathbf{P}, \quad (13)$$

where \mathbf{M} , \mathbf{C} and \mathbf{K} are the global mass, damping and stiffness matrices of the track respectively; $\mathbf{K} = \mathbf{K}_r + \mathbf{K}_p$, where \mathbf{K}_r is the contribution from the rail bending stiffness and \mathbf{K}_p contains the nonlinear railpad stiffnesses. The external load is contained in the vector \mathbf{P} . Note that Hermitian interpolation functions are used to convert the input force onto equivalent nodal forces. The solution of Eq. (13) is obtained by numerical integration [7]. Once the displacement, velocity and acceleration vectors have been computed, the reaction forces in the railpads can be computed, in the space-time domain, as a sum of the stiffness and damping forces as follows

$$\mathbf{F}_t(x, t) = \mathbf{C}\dot{\mathbf{U}}_p + \mathbf{K}_p\mathbf{U}_p, \quad (14)$$

where \mathbf{U}_p and $\dot{\mathbf{U}}_p$ are respectively the displacement and velocity vectors of the rail at the fastener positions. Hence, \mathbf{F}_t has size $(2N_p + 1) \times N_t$, where N_p is the number of railpads on either side of $x = 0$ and N_t is the number of time steps.

The spatial Fourier transform of \mathbf{F}_t to the wavenumber domain can be obtained from

$$\hat{\mathbf{F}}_t(\xi, t) = \sum_{q=-N_p}^{N_p} \int_{-\infty}^{\infty} \mathbf{F}_{t_q}(t) \delta(x - x_q + vt) e^{-i\xi x} dx, \quad (15)$$

where $x_q - vt$ corresponds to the positions of the railpads in the moving frame of reference. Therefore

$$\hat{\mathbf{F}}_t(\xi, t) = \sum_{q=1}^{N_p} \mathbf{F}_{t_q}(t) e^{-i\xi(x_q - vt)}. \quad (16)$$

Similarly, the temporal Fourier transformation of $\hat{\mathbf{F}}_t(\xi, t)$ to the frequency domain, at the excitation frequency, can be calculated as

$$\hat{\mathbf{F}}_t(\xi, \omega) = \sum_{q=1}^{N_p} \int_{-\infty}^{\infty} \mathbf{F}_{t_q}(t) e^{-i(\xi x_q + (\omega_0 - \xi v)t)} dt, \quad \text{for } \omega = \omega_0. \quad (17)$$

Equation (17) gives the reaction force in the wavenumber domain corresponding to the excitation frequency, i.e. $\hat{\mathbf{F}}_t(\xi, \omega_0) = \hat{\mathbf{F}}_t(\xi)|_{\omega=\omega_0}$. This can then be substituted in Eq. (11) to calculate the interaction force at the slab-ground interface and subsequently ground vibration.

3. Results and discussion

Table 1 contains the track and soil parameters used in this study. The slab pad is made very stiff with $K_{sg} = 3.5 \times 10^6$ MN/m² and $C_{sg} = 7.28$ MNs/m². Additionally, the empirical relationships and parameter values for the preload dependent railpad properties can be found in [2]. All the results presented in this work account for two rails acting on the slab.

Table 1: Track and soil parameters used in the numerical examples

Track parameters		Soil parameters	
Mass of rail, M_r	60.21 kg/m	Density, ρ	1800 kg/m ³
Mass of slab, M_s	3500 kg/m	Pressure wave speed, c_1	400 m/s
Bending stiffness of rail, EI_r	6.4 MN m ²	Shear wave speed, c_2	200 m/s
Bending stiffness of rail, EI_s	1430 MN m ²	Rayleigh wave speed	183 m/s
Linear railpad stiffness, K_{rs}	33.33 MN/m ²	Poisson's ratio	0.33
Railpad damping factor, C_{rs}	24.43 kNs/m ²	Damping ratio	0.05

Results are first presented to check the validity of the weak coupling assumption against the strong coupling case for linear parameters. In the FE model, a linear case is achieved by setting the preload to zero.

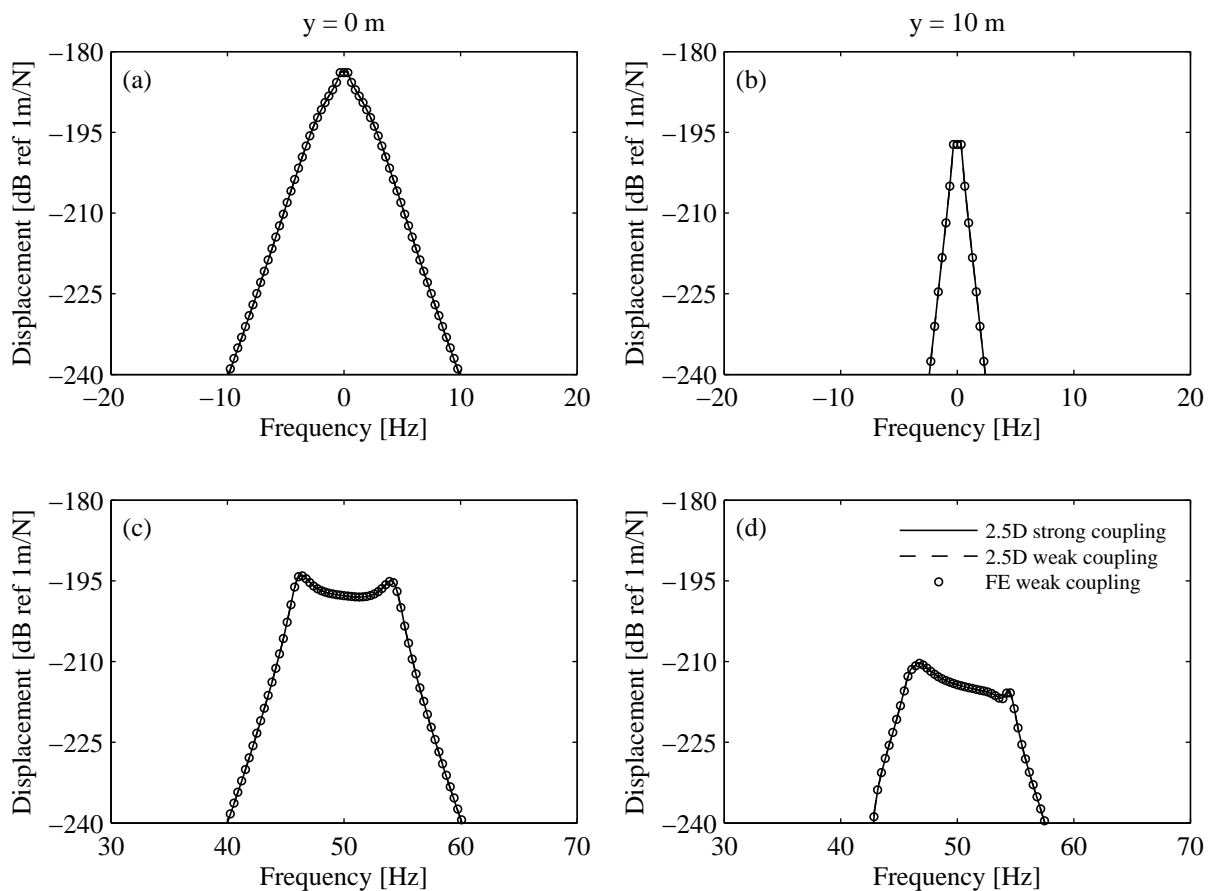


Figure 2: Displacement of a point on the ground due to a load moving at 120 km/h and oscillating at (a-b) 0 Hz and (c-d) 50 Hz. Comparison of the three cases for linear parameters

Fig. 2 shows the displacement spectra for two points on the ground at $y = 0$ and 10 m, due to a load moving on the track at 120 km/h and oscillating at 0 Hz for (a-b) and 50 Hz for (c-d). In all cases, the results from the FE model agree well with those from the weakly and strongly coupled 2.5D models. For the non-oscillating load case in (a-b), the response is symmetrical about 0 Hz since there is no Doppler effect, since the load speed is much lower than the lowest wave speed of the ground. For the oscillating load case in (c-d), on the other hand, this effect is apparent. The peaks in the displacement correspond to the Doppler shifted excitation frequency, $\bar{f} = (\bar{c}/(\bar{c} \pm v))f_0$, as the load approaches and leaves the observation point; where \bar{c} is the speed of the propagating waves. When the Rayleigh wave speed on the ground is used, this results in frequencies of 42 Hz and 61 Hz. However, the bending stiffness of the slab contributes to the overall stiffness of the slab-ground system and the peaks appear at 46 Hz and 54 Hz, corresponding to an equivalent ground with wave speed of about 435 m/s.

Results will now be presented for the nonlinear model for three preload levels; 0, 75 and 125 kN, individually applied on each rail. The results given here are the dynamic parts, with the static preload used for the calculation of the loaded stiffness and damping properties as outlined in [2].

Fig. 3(a) shows the time history of the transmitted force in the railpad at the centre of the track due to a harmonic load with $f_0 = 50$ Hz and $v = 120$ km/h. The corresponding force in the wavenumber domain for all railpads is shown in (b). The maximum loaded stiffnesses of the

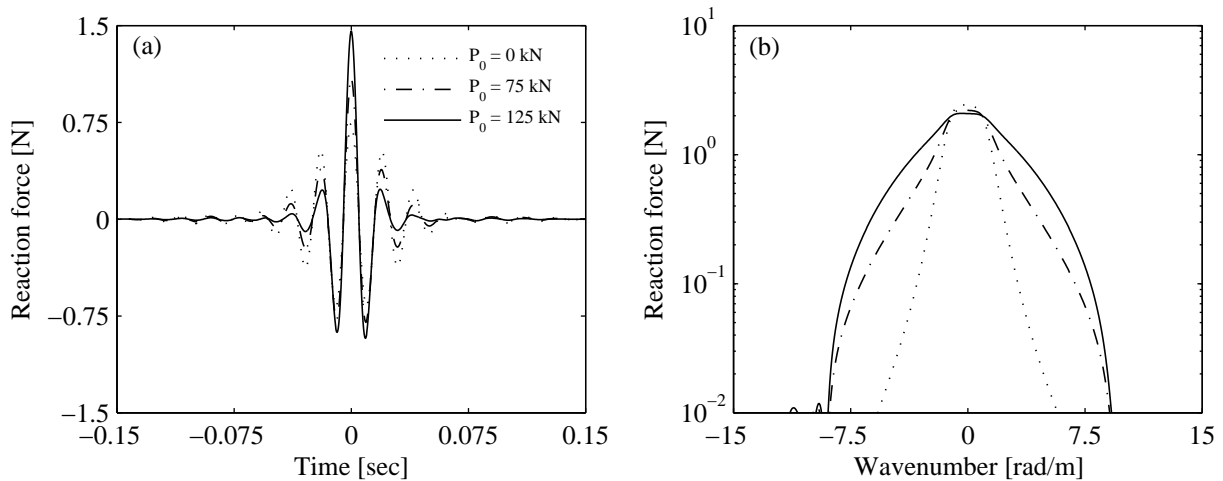


Figure 3: (a) Reaction force time histories for the middle railpad (b) reaction force for all railpads in the wavenumber domain, due to a unit load with $f_0 = 50$ Hz and $v = 120$ km/h

railpad are 54 and 164 MN/m for the 75 and 125 kN preloads respectively, compared with 20 MN/m for the linear case. The increased stiffness of the railpads induced by the preload results in larger amplitudes of the transmitted force with an accompanying increase in the decay rates, as shown in (a). The wavenumber domain plot in (b), however, shows slightly lower amplitudes around the zero wavenumber for increasing preload levels. This means that the total force transmitted to the ground from all railpads, is greater for the softer railpads, since the forces spread over a much wider region. The opposite effect is observed away from the zero wavenumber.

Fig. 4 shows the maximum space-time domain displacements of the ground at (a) $y = 0$ m and (b) $y = 10$ m, plotted as a function of excitation frequency for a load moving at 120 km/h. For each excitation frequency, the displacement of the ground in the space domain is calculated by taking the inverse Fourier transform of $\hat{U}_g(\xi, y)$ from the ξ to the x domain and the maximum absolute value recorded. The observation in Fig. 3(b) is evident here, as the linear case shows higher amplitudes of ground vibration for most of the frequency range. At higher frequencies, however, the nonlinear cases exhibit larger peak displacements. The maximum differences in the amplitudes is limited to 6 dB for

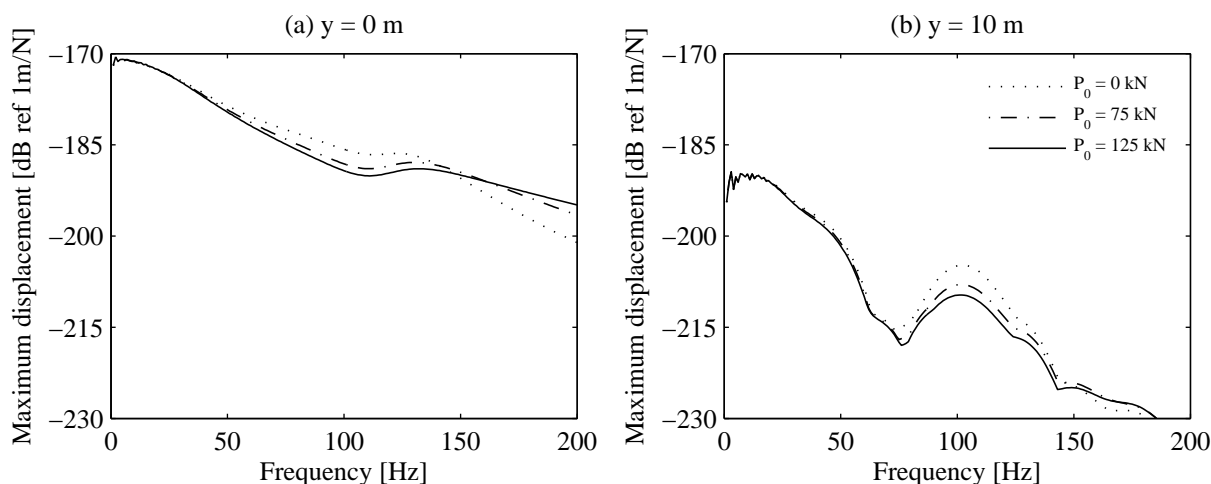


Figure 4: Maximum space-time domain displacements of a point on the ground, plotted against excitation frequency for a unit oscillating load moving at 120 km/h. Comparison for three preload levels

the range of frequency shown.

4. Conclusions

This paper investigates the effect of nonlinearity of railpads on ground borne vibration. The railway track is formulated in the time domain for the calculation of the forces transmitted through the railpads. These are then transformed to the wavenumber domain and applied to a separate linear slab-ground model using a weak coupling approach. This approach is validated against a strong coupling formulation for linear parameters. It can be summarised that the inclusion of railpad nonlinearity into the modelling results in differences in peak displacement amplitudes of up to 6 dB over a frequency range of 0-200 Hz, compared with the corresponding linear case, for the parameters used in this work.

Acknowledgement

This work is undertaken as part of the MOTIV (Modelling of Train Induced Vibration) project which is funded by the EPSRC under grant EP/K005847/2.

References

- ¹ T.X. Wu and D.J. Thompson. The effects of local preload on the foundation stiffness and vertical vibration of railway track. *Journal of Sound and Vibration*, **219**(5):881–904, (1999).
- ² S.G. Koroma, M.F.M. Hussein, and J.S. Owen. The effects of railpad nonlinearity on the dynamic behaviour of railway tracks. In *Proceedings of the Institute of Acoustics (Acoustics 2013), Volume 35 Pt. 1*, (2013).
- ³ S.G. Koroma, M.F.M. Hussein, and J.S. Owen. The effects of railpad nonlinearity on the vibration of railway tracks under a harmonic load. In *Proceedings of the 11th International Conference on Vibration Problems (ICOVP-2013), Lisbon, Portugal, 9-12 September*, (2013).
- ⁴ S.G. Koroma. *Vibration of beams on non-linear and non-homogeneous elastic foundations with application to railway tracks*. PhD thesis, University of Nottingham, (2014).
- ⁵ X. Sheng, C.J.C. Jones, and M. Petyt. Ground vibration generated by a load moving along a railway track. *Journal of Sound and Vibration*, **228**(1):129–156, (1999).
- ⁶ K.F. Graff. *Wave Motion in Elastic Solids*. Dover publications, inc., New York, (1991).
- ⁷ K-J Bathe and M.M.I. Baig. On a composite implicit time integration procedure for nonlinear dynamics. *Computers & Structures*, **83**:2513–2524, (2005).